Marine Geology, 116 (1994) 37–56
Elsevier Science B.V., Amsterdam

Propagating rift and overlapping spreading center in the North Fiji Basin

Etienne Ruellan[a], Philippe Huchon[b], Jean-Marie Auzende[c,1] and Eulàlia Gràcia[c]

[a]*CNRS, URA 1279 Géodynamique, rue A. Einstein, Sophia Antipolis, F-06560 Valbonne, France*
[b]*CNRS, URA 1316, Laboratoire de Géologie, ENS, 24 rue Lhomond, F-75231 Paris Cedex 05, France*
[c]*IFREMER, DRO-GM, B.P. 70, F-29280 Plouzané, France*

(Received May 6, 1993; revision accepted July 29, 1993)

ABSTRACT

Ruellan, E., Huchon, P., Auzende, J.-M. and Gràcia, E., 1994. Propagating rift and overlapping spreading center in the North Fiji Basin. In: J.-M. Auzende and T. Urabe (Editors), North Fiji Basin: STARMER French–Japanese Program. *Mar. Geol.*, 116: 37–56.

The present day geometry of the North Fiji marginal basin, at the Pacific and Indo-Australian plate boundary, results from a polyphased tectonic evolution. Since the beginning of the opening, spreading occurred along several ridge axes that are characterized by highly variable trends. From 15°S to 21°40′S, the present day trends of the axis are mainly N20°W, N20°E and N–N5°E.

The structural analysis of multi-beam echo sounder and seismic data combined with submersible observations (18 dives in this area) allow a precise study of relationships between the N–N5°E and N20°E axes near 18°30′S. Two main oceanic features occur in this area. The most striking one consists in a broad northward propagating rift of the N–N5°E spreading ridge. The northern tip of the propagator is located at 18°10′S, on 173°30′E and is characterized by a northern V-shaped end and a slight camber. The diving observations corroborate the present day magmatic and tectonic activities along the N–N5°E spreading axis located between 18°10′S and 20°30′S and its northward propagation to the detriment of the N20°E axis which is less active at its southern end. Moreover, the youngest axis trends, inside the N20°E axial domain, confirms this northward propagation of the N–N5°E structural trends. The N–N5°E spreading axis shows very close similarities with those of an intermediate to fast-spreading ridge, either in its morphology or in its spreading rate. On the other hand, the N20°E axis displays a large tectonically active overlapping arm, that is counterposed to the northern end of the N–N5°E propagating system. The transform zone between the two overlapping arms is characterized by typical oblique and curved structural patterns in the sea floor. The whole tectonic system constitutes thus a typical large overlapping spreading center. The average propagating rate is calculated at 5.7 cm/yr that is compatible with backward migration of the N20°E overlapping arm.

This study confirms the high instability of the North Fiji Basin spreading system through time and space, due to the regional tectonic stress produced by the plate convergence and the double sphenochasmic opening of the basin.

Introduction

Spreading discontinuities, such as propagating rifts and overlapping spreading centers (OSC) occur in many places along divergent plate boundaries. Most of these transform features have been described, at various scales, on the main spreading oceanic ridges, with either low, intermediate or fast spreading rates (Shih and Molnar, 1975; Hey, 1977; Schilling et al.; 1982; Mac Donald and Fox, 1983; Mac Donald, 1989; Mac Donald et al., 1991; Gente, 1987; Kleinrock and Hey, 1989).

These discontinuities are generally interpreted as unsteady and transient phenomena related to geometric rearrangements of the ridge axis segmentation through space and time. Whether these rearrangements are related to a change in the spreading orientation or to propagation into an older oceanic crust is partly controversial (Menard and Atwater, 1968, 1969; Hey et al., 1988). The oceanic propagators are considered to be the result

[1]Present address: ORSTOM, UR 1F, B.P. A5, Nouméa Cedex, New Caledonia

0025-3227/94/$07.00
SSDI 0025-3227(93)E0094-M

of lengthening by the propagation of a spreading axis into old or recently formed pre-existing lithosphere, that takes over plate separation from another axis. Consequently, there is a transfer of lithosphere from one plate to another (Kleinrock and Hey, 1989).

The North Fiji Basin (NFB hereafter), in the Southwest Pacific (Fig. 1), represents a new site for the investigation of propagating rifts, OSC's and triple junctions since its recent tectonic evolution is characterized by many reorientations of the spreading geometries in the last few million years (Auzende et al., 1988b; Lafoy, 1989; Ruellan et al., 1990, 1992; De Alteriis et al., 1993).

The purpose of this paper is to describe and analyse the detailed morphology and the tectonic development of the central N–N5°E and N20° to N15°E segments (N20°E hereafter) of the North Fiji Basin ridge between 17°S and 21°S, that show similarities with those of main ocean intermediate to fast spreading ridges. The recent tectonic evolution of this sector of the NFB ridge is characterized by a northward propagation during the last 1.8 Ma, since anomaly 2 (1.67–1.87 Ma; Vine and Matthews, 1963; 1.65–1.88 Ma; Harland et al., 1990) which is the older magnetic anomaly attached to the propagating system (see later).

Methods

Interpretations presented in this work are based on a detailed analysis of geological and geophysical data (Fig. 2) collected within SEAPSO project (1985–1986) and French–Japanese joint program STARMER (1987–1991) The data set includes multi-narrow-beam echo-sounding, seismic reflection and magnetic surveys, and deep tow photographs and video obtained during *Seapso* 85, *Kaiyo* 87, 88 and 89 and *Yokosuka* 90 and 91 cruises. Eighteen dives have been conducted with the manned submersibles *Nautile* and *Shinkai* and with the *Dolphin* ROV on three sites along the N–S

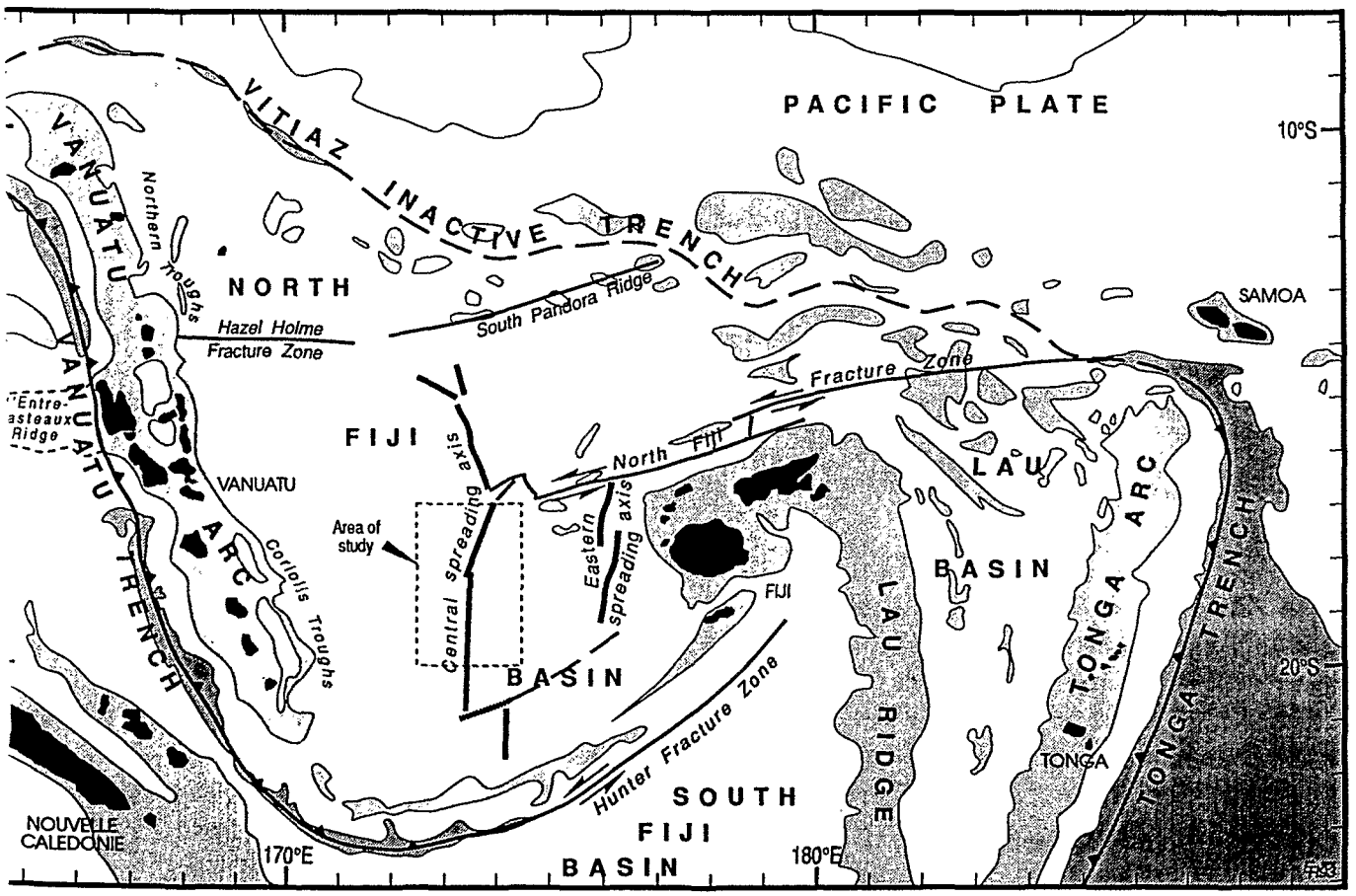

Fig. 1. Geodynamic setting of the North Fiji Basin. N–S, N20°E and N20°W are the main segments of the ridge axis.

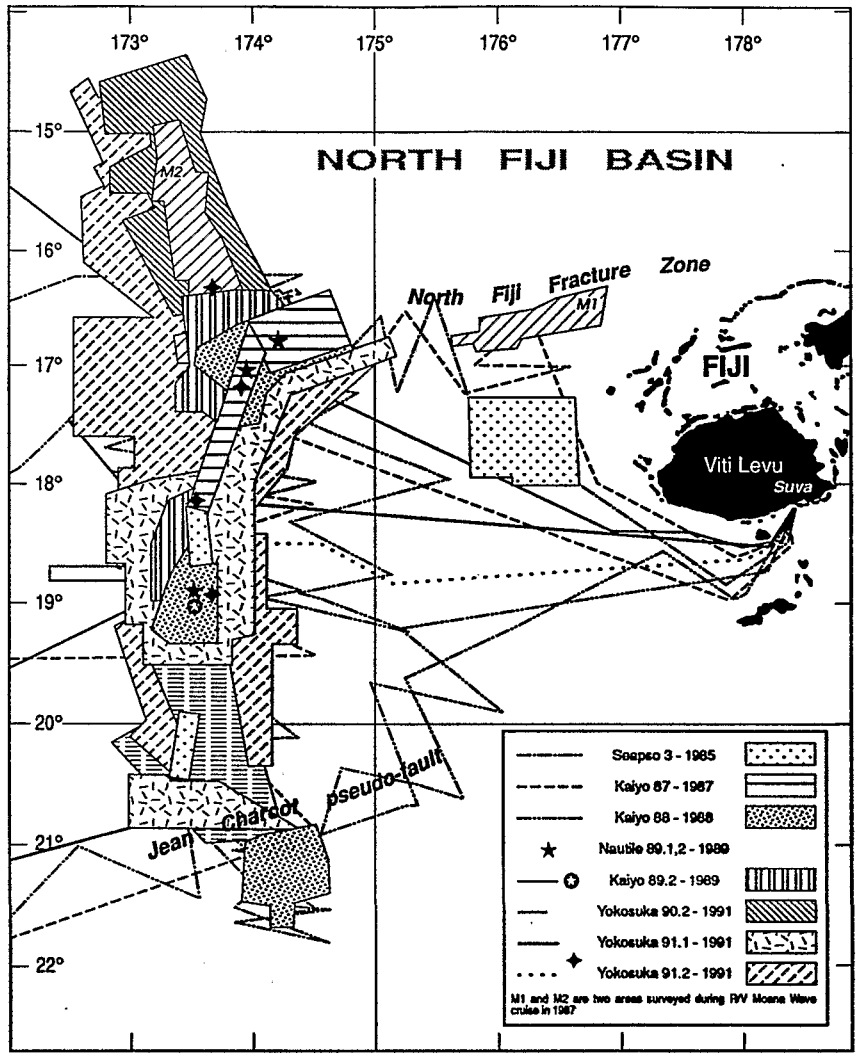

Fig. 2. The SEAPSO and STARMER surveys in the NFB since 1985. The frames indicate the 60% to full multibeam coverage.

(station 14) and N20°E (stations 4 and 6) ridges during *Starmer* 89, *Kaiyo* 89 and *Yokosuka* 91 cruises.

Multi-narrow-beam survey

The extensive bathymetric data set was collected using three different swath-mapping multi-narrow-beam sonar systems, the Seabeam (16 beams) (Renard et Allenou, 1979) on board the french R/V *Jean Charcot* (1985), the Seabeam on board the Japanese R/V *Kaiyo* (1987, 1988, 1989), and the Furuno HS-10, a Japanese swath-mapping multi-narrow-beam sonar (45 beams), on board the Japanese R/V *Yokosuka* (1991).

The 50% to full coverage multi-narrow-beam echo sounding extends on the whole ridge domain for more than 800 km along strike and for about 100 km in width. It is probably one of the most comprehensive swath-mapping of a ridge axis ever done (Fig. 2). The navigation was based on Global Positioning System (GPS) for about 60% of the survey and accurate transit satellite fixes otherwise. Therefore no navigation corrections were assumed necessary. This was justified by the absence of any significant discrepancies at track crossings.

In our study, the mesh size of the sampling grid, used to build the bathymetric Digital Elevation Model (DEM) (Fig. 3) and the 3-D view (Fig. 4) of the central axis of the NFB, was chosen in order to slightly under-sample the original data rather than to over-sample them. Therefore the difficult problem of interpolation in the case of non-homogenous data was bypassed. The scale of

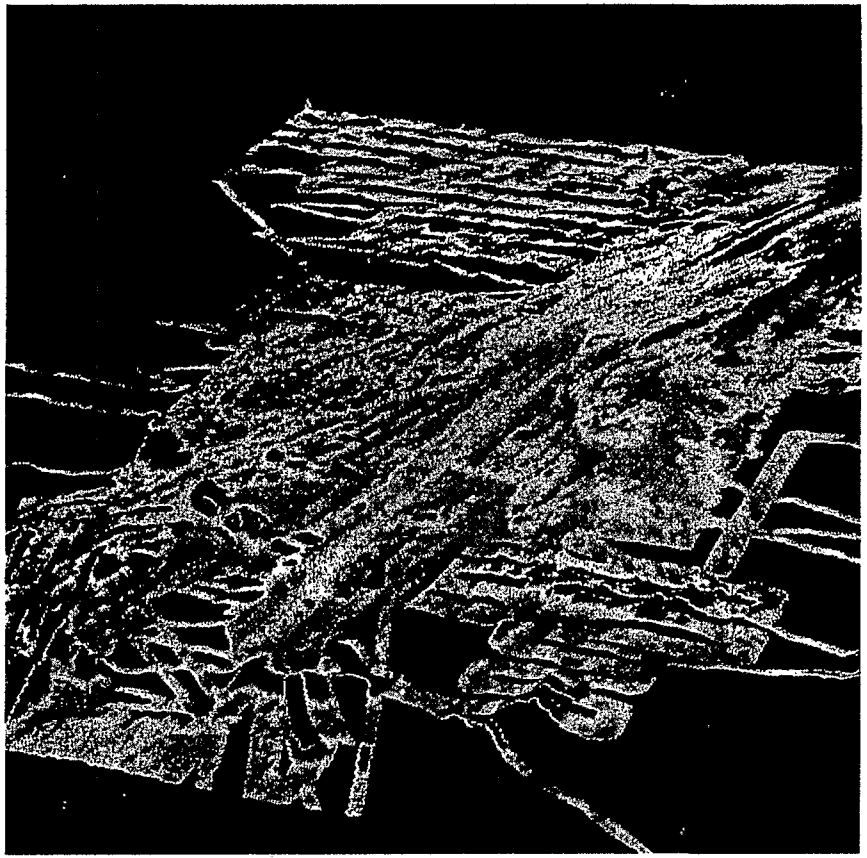

Fig. 4. 3-D view of the digital elevation model (DEM) of the NFB spreading ridge (Ifo–Khoros–Istar processing).

Fig. 3. Detailed multibeam bathymetry of the ridge between 17°S and 20°S. The contour interval is 100 m.

the map produced is 0.002° per pixel, thus 1 pixel represents about 222 meters. The last data also provide parameters to trace the ray-path of the sound at each measurement point and to compute a refraction correction along the salt/temperature water layers, using a 10 layer model.

The grid is filled by reading the data sequentially, cruise after cruise in their chronological order. When a node is encountered that already has a data value the newer value is substituted because it is assumed that navigation uncertainties and measurement accuracy have been improved in the more recent cruises. Such a procedure corresponds roughly to a random under-sampling of an over-sampled data set. A random selection preserves high frequency variations, rather than averaging the multiple data, which would cause an unsuitable smoothing of the DEM, which in turn would cause a significant restriction in the detection of fault scarps. Certainly, the systematic choice of the most recent data is only a rough approximation to a random selection, but the major defect is to give priority to the most recent cruise which as we have said is likely to be the most accurately positioned. Thus the chronological criterion, determining the sampling order within a single cruise, results in enough complex circumstances for the sampling to be considered as random.

Seismic survey

At the same time, a comprehensive single channel seismic survey was carried out in the North Fiji Basin during SEAPSO and STARMER projects in order to improve the structural knowledge of the oceanic bottom. Most of the profiles are single channel analogous seismic reflection profiles obtained with air guns.

Magnetic surveys

During most parts of the bathymetric survey, the total magnetic field was measured using a proton precession magnetometer towed 200 to 300 m behind the ship. After processing described elsewhere (Huchon et al., 1994-this issue), the data were used to draw magnetic anomaly profiles projected along tracks (Fig. 6) in order to identify magnetic lineations and infer a tentative age for the oceanic crust.

Deep-sea observations

Two methods were used to obtain the deep-sea observations data set. First, ocean bottom photographs and video were obtained during the *Kaiyo* 87, 88 and 89 cruises using a deep-towed vehicle which allowed observation of the ocean bottom in real time by video, bottom photography, and conductivity, salinity and temperature measurements as well as water depth.

Second, twenty three dives, 3 with *Nautile*, 18 with *Shinkai* 6500 and 2 with *Dolphin* 3K ROV, were conducted on the N–S (station 14) and on the N20°E (station 6) spreading axes during *Starmer* II-89, *Kaiyo* 89 and *Yokosuka* 91 cruises.

Geodynamic setting

The North Fiji Basin (Southwest Pacific) is a triangular shaped marginal basin that opened recently along the Pacific and Indo-Australian plate boundary (Fig. 1). It is delimited by the active New Hebrides island arc and subduction zone to the west, the Fiji Islands platform to the east, the inactive Vitiaz subduction zone to the north and the Matthew–Hunter ridge and the Hunter fracture zone to the south.

The present day geometry of the North Fiji Basin results from a multiphase tectonic evolution since the beginning of the spreading in the Late Miocene (~10 Ma). The oceanic opening of the basin is generally considered to be linked with the rotation of two tectonic elements: the clockwise rotation of the New Hebrides volcanic arc system and the counter-clockwise rotation of the Fiji platform (Chase, 1971; Gill and Gorton, 1973).

These movements imply a complex evolution of the basin's accretionary system, with multiple severe reorientations in the geometry of the spreading axis during the last 10 Ma. Since the beginning of the opening, spreading occurred along several ridge axes that are characterized by highly variable trends: N40°–30°W, N, N20°E, N20°W, N60°W (?) and N80°–90°W (?). The N40°–30°W trend of the spreading axis which was active during the first

stage of opening can be deduced from magnetic data and to a lesser extent from bathymetric data. In the last 3.5 Ma, a roughly N–S trending spreading ridge system has developed in the central and southern parts of the basin, superimposed on older N30°W lineations (Auzende et al., 1988b). The present day active spreading system, from 14°30′S to 21°40′S (Fig. 1), consists of four differently oriented radix segments; two of them are beleived to converge with the left lateral North Fiji fracture zone to constitute the 16°50′S triple junction (Lafoy et al., 1987, 1990; Auzende et al., 1990). From 14°30′S to the triple junction area, a 250 km long N20°W trending spreading axis has developed since about 1 Ma (Gràcia, 1991). Between the triple junction and 18°30′S, the 175 km long N20°E spreading axis has also developed since about 1 Ma. The N to N5°E trending spreading ridge, from 18°10′S to 20°30′S with an approximate length of 280 km (Auzende et al., 1988a,b), is at least 3 Ma old. South of 20°30′S, the southernmost N–S spreading system is offset by about 80 km to the east from the previous N–S ridge through a wide N45°E to N60°E pseudofault (Maillet et al., 1986; Ruellan et al., 1989); its length is about 50–200 km.

Tectonics of the central part of the North Fiji Basin

A 3-D view of the detailed bathymetry of the spreading ridge domain south of triple junction is presented in Fig. 4. The map (Fig. 3) results from a compilation of the whole set of data obtained during SEAPSO and STARMER projects (Fig. 2). Structural analysis of multi-narrow-beam echo sounder and seismic data combined with submersible observations allow a detailed study of relationships between the N–N5°E and N20°E axes near 18°30′S, where a spectacular propagating rift occurs. The tectonic lineaments chart resulting from this study is shown in Fig. 5.

Five domains each defined by a set of parallel lineations have been identified in the study area (Figs. 5 and 9); two of these, which are related to the currently active North Fiji Basin spreading axis, are:

– a N20°E domain to the north contains lineations parallel to the present N20°E axis;

– a N to N5°E domain to the south (which comprises the propagating rift) contains lineations parallel to N–N5°E axis, inside the V-shaped region on either side of the axis;

The other three, which are older, are:

– a N30°W domain east of the V-shaped region;

– a N–S domain northeast of the propagating rift;

– and a N30°E very complex domain with concave eastward structural trends west of the N20°E domain.

The magnetic anomaly pattern (Fig. 6) partly reflects this complexity. The axial anomaly is well defined in the N–S to N5°E domain. It shows an increase in amplitude toward the tip of the propagating rift, which is the typical signature of the FeTi enriched basalts formed in this context (Miller and Hey, 1986). South of 19°S, anomalies J and 2 can be identified (Fig. 6). It leads to a full spreading rate of about 7 cm/yr, a value which is slightly lower than the one measured at 20°S (7.6 cm/yr, Huchon et al., 1994-this issue). Note that a rate of 5.6 cm/yr was measured by Auzende et al. (1990) at 18°30′S, but it is located inside the propagating rift and thus does not represent the total spreading rate at this latitude. Between 19°S and 18°S, the identification of magnetic anomalies becomes less reliable, although clear lineations appears on the map. Further north, in the N20°E domain, the axial anomaly appears to be flanked by anomaly J, giving a full spreading rate of about 5.9 cm/yr at 17°30′S for the last one million years (Huchon et al., 1994-this issue). This spreading rate is significantly lower that the rate measured at 19°20′S, showing an overall northward decrease in spreading rate approaching the 16°50′S triple junction.

The active North Fiji Basin spreading axis

The N20°E ridge axis domain

The N20°E segment of the NFB spreading axis extends, for at least 175 km, from 16°50′S, where a large oceanic build-up occurs in the triple junction area, to the intersection with the N–S axis near 18°30′S (Figs. 3 and 4). It is underlined by structural lineations trending N15°E to N25°E. This pattern is concentrated in a 75 km wide belt that is superimposed on older external structural

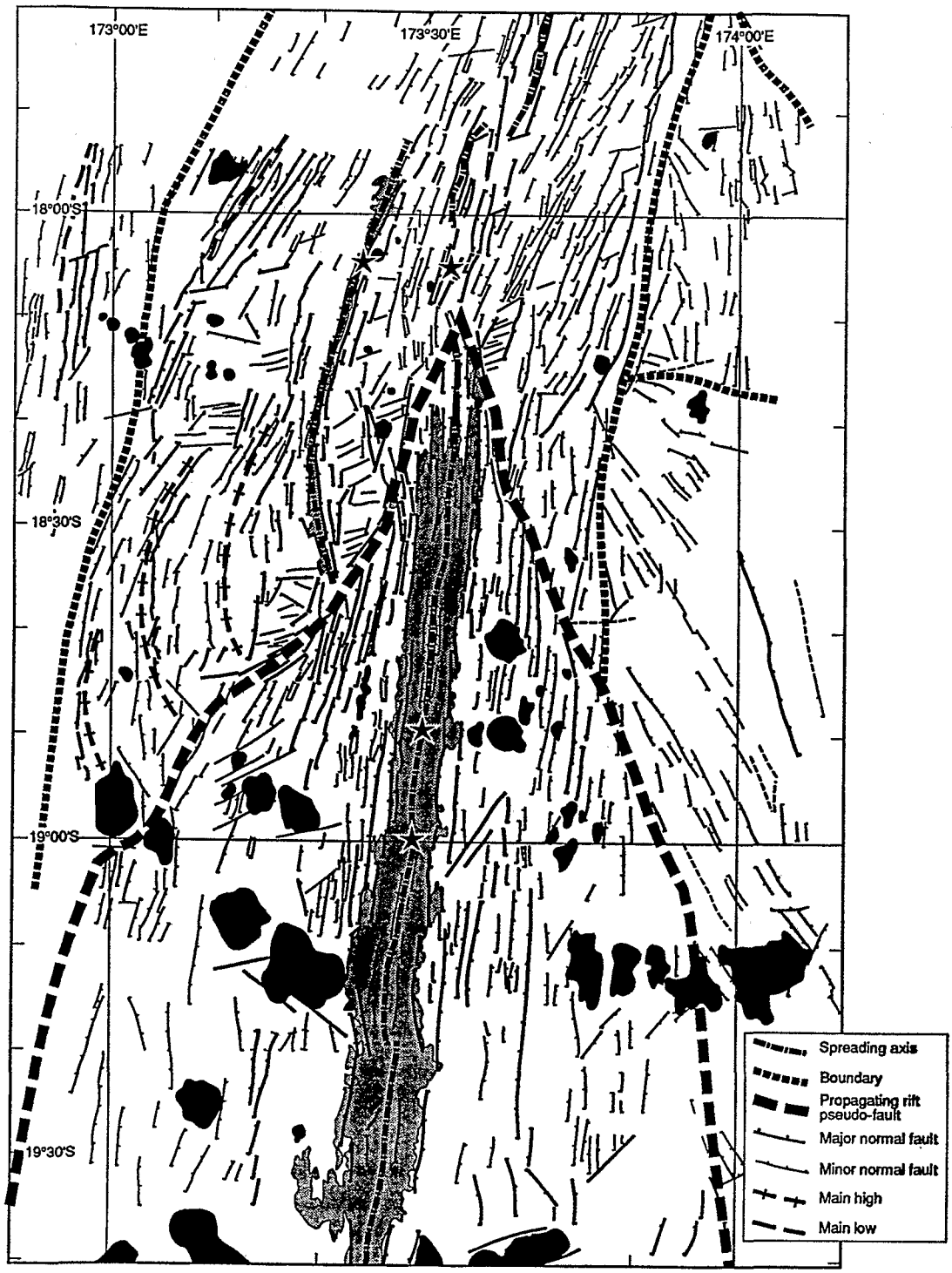

Fig. 5. Major tectonic lineaments of N20°E and N–S segments, between 17°S and 20°S. Stars indicate the diving sites and off-axis volcanoes appear in black.

trends which are either N30°W, N–S or N35°E (Figs. 3 and 5).

The present day active N20°E spreading axis is divided into three second order segments.

North of 17°51'S, the axial morphology is represented by a N15°E double ridge, about 10 km wide, which rises some 200–300 m above abyssal plain and is splitted by an elongated graben, 2 to 5 km wide. This axial topography deepens southward (Fig. 8) and can be easily identified from

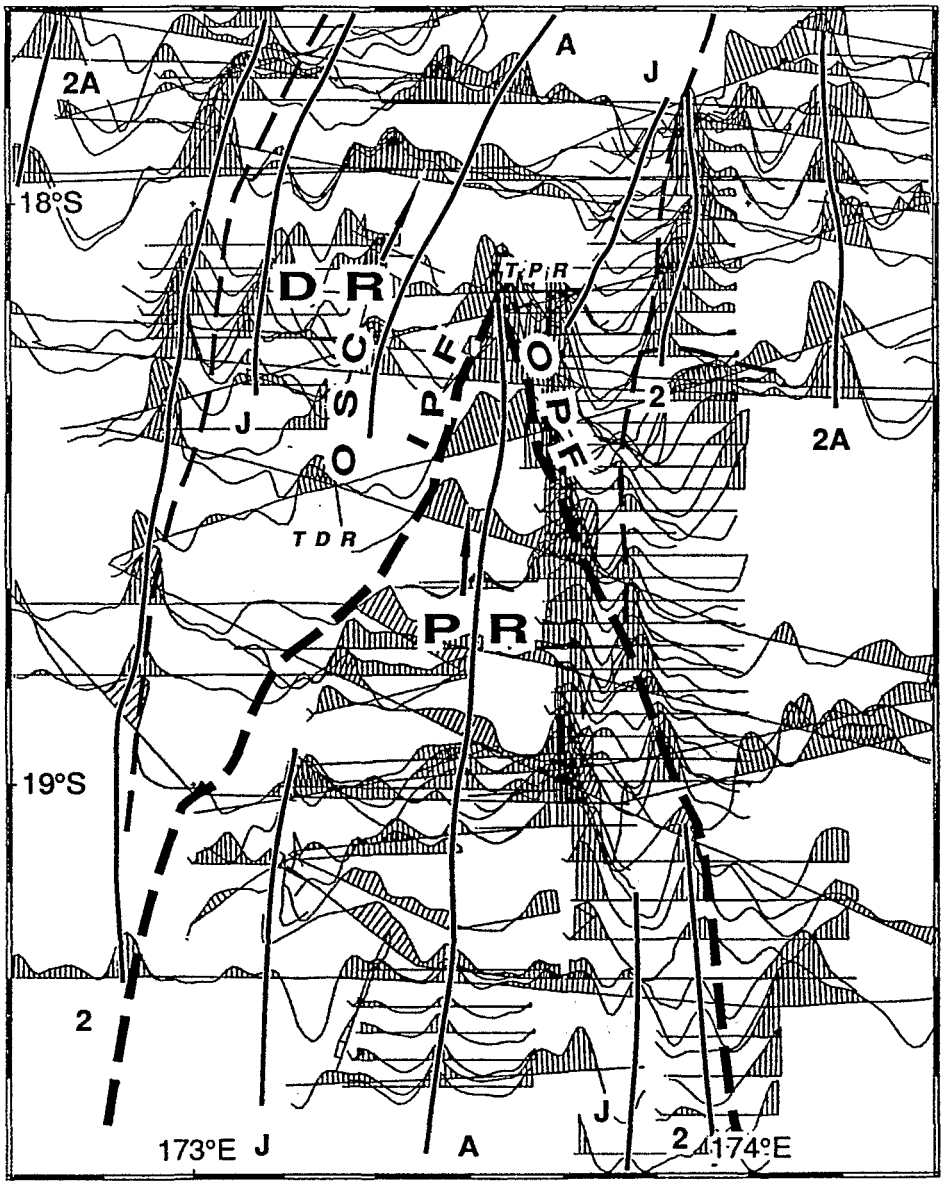

ig. 6. Magnetic anomalies along profiles across N–N5°E and N20°E axes. Note the differently oriented lineations north of the ropagating rift pseudo-faults and the asymmetry of the anomalies south of them.

athymetry (Fig. 3) up to about 17°51'S. The orthern part of the segment shows two large, 600m deep symmetrical grabens on each side of ne 40 km long, 15 km wide axial ridge, with an xternal slightly curved shape. The location of the resent axis with respect to the grabens is slightly ccentric. This topography is quite anomalous hen compared with Pacific ridges; for Lafoy et al. 1990), it suggests a magmatic phase alternated ith tectonism.

Between 17°51'S and 18°10'S, the location of the xis becomes more difficult to identify since bottom eatures are being disturbed at the junction with the N–S segment of the spreading axis and by many small off ridge volcanoes. The spreading center jumps en echelon twice westward becoming an elongated and narrow ridge, trending N15°E and rising up to 2600 m depth, at the southern end.

Four submersible dives using the *Shinkai* 6500 have explored the southern tip of the N20°E segment of the NFB spreading axis (Fig. 7), along a nearly E–W cross section located between 18°03'S and 18°07'S and between 173°24'E and 173°34'E. The depth ranges from 3000 to 2600 m.

In this area, the spreading ridge is not so clearly identified as in the northern part of the N20°E

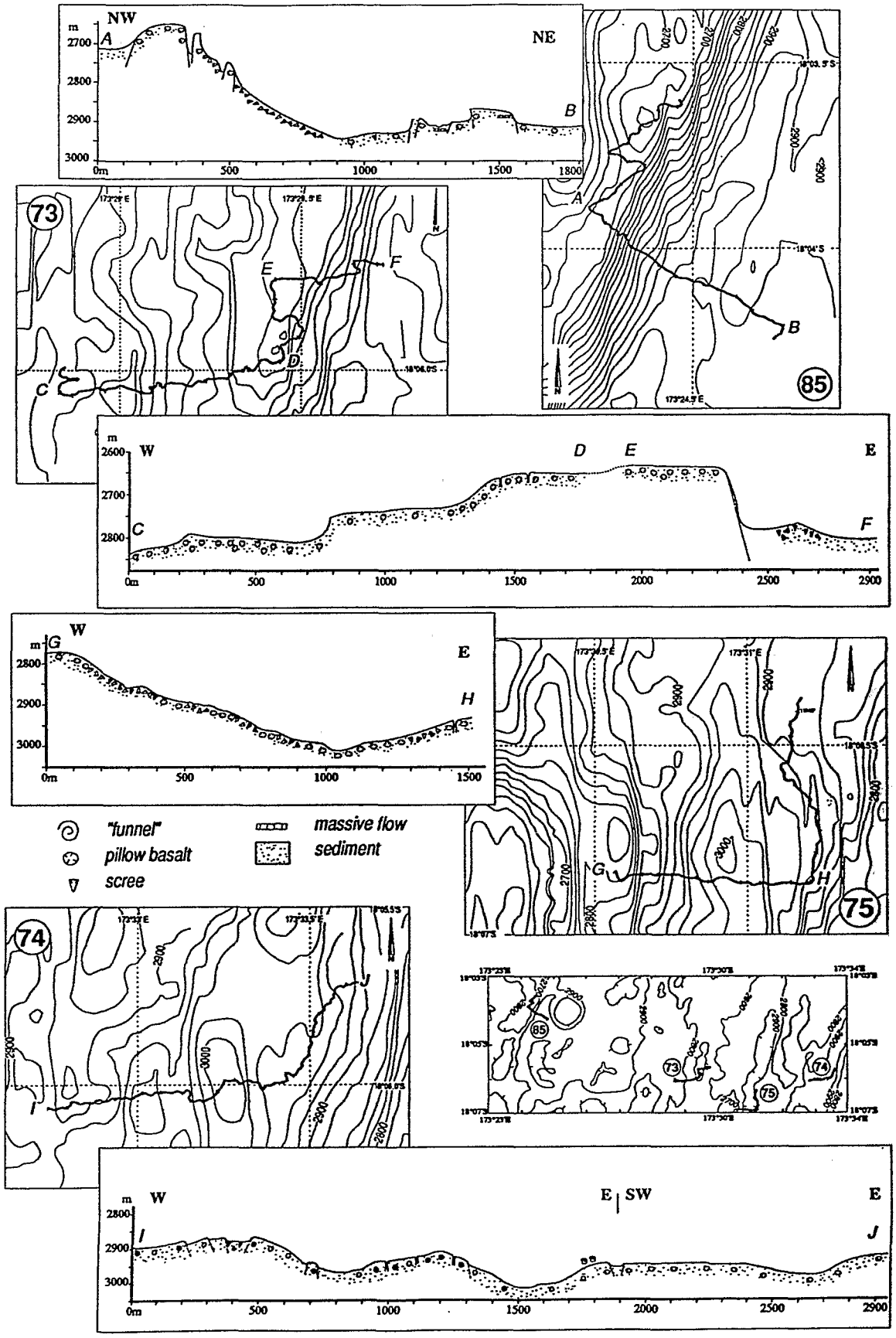

Fig. 7. Geological cross sections from dives at station 6 (with help of H. Ondréas).

axis. The large scale structural pattern is dominated by a succession of parallel horsts and grabens. During the *Kaiyo* 87 cruise, a very high manganese anomaly was detected at station 6. Here, the N20°E trending ridge to the north clearly overlaps with N–N5°E ridge to the south. The manganese anomaly seems to coincide with the location of the axis of the former one. Station 6 therefore presents an excellent opportunity to explore the relationships between tectonism, hydrothermalism and petrology on overlapping ridges close to the junction between the two spreading axes.

From diving observations at station 6, the sea bottom is strongly covered by rather thick sediments (10 cm to few meters), except on the western ridge (dive 85). Eastward, from the bathymetry, the bottom is not much disturbed by tectonic activity like fissuring, faulting, and mechanical brecciation. But, the detailed morphology observed during the dives 73, 74 and 75 is more complex and rather different from the one given by the multi-narrow-beam bathymetric map. The tectonic features observed during dives consist mainly of N to N10°E open faults, 1–5 m wide and 10–15 m deep. Westward, the cross section made during the dive 85 shows three main areas from west to east. (1) The first structural area is located at the top of the main western ridge. The sedimentary cover thickens rapidly over the western slope. The northwestern side of the ridge crest becomes a steep west-facing fault cliff, about 30 m high, consisting of basalt pillow lavas and lava flows of different ages and crosscut by many more or less opened N20°E fractures. (2) The second structural area is a very steep east-facing, N20°E trending fault escarpment, which is delineated by three main vertical fault scarps, steep antithetic faults steps, and very narrow and elongated horsts and grabens, without any sedimentary cover. These observations indicate tectonic seems to be very active in this area. We found many large fresh screes at the foot of the scarps as the result of this tectonic activity. The main scree lies at the foot of the main cliff and covers about half of it. (3) At the foot of the fault scarp, the third area displays a rather smooth topography, according to the bathymetric survey. In fact, the sea floor is made of a succession of eastward tilted half horsts and grabens. bounded by five 10 to 30 m high fault cliffs, mainly west-facing. The whole area is covered by rather flat lying unconsolidated sediment. The basalt pillow lavas crop out mainly along the crests of the tilted blocks and along the fault cliffs, which trend mainly N20°E.

As described before in the whole diving area at station 6, the oceanic basement generally crops out along 5 to 15 m high, N10° to N20°E trending scarps resulting from normal faulting and block tilting, and on small scattered seamounts. Basement consists of unbroken basalt pillow lavas commonly with finger-like spines prograding about 10 cm from the surface of pillows, of tubular and round pillow lavas, of massive lava flows (above pillows) and of scree. We noticed that the bottom water was sometimes turbid, especially along the high east facing fault cliff of the western ridge, suggesting hydrothermal activity. But no temperature anomaly or any other sign of hydrothermal activity was detected anywhere.

The fact that the central and eastern area are covered by rather thick recent soft sediments clearly indicates that the area did not undergo recent magmatic activity and underscores a discontinuity in the spreading processes between the N20°E and N–N5°E active spreading ridges. The entire area of station 6 displays features characterizing a predominance of tectonic activity over the magmatic one. The structural analysis of the new multi-narrow-beam echo-sounder data set (Ruellan et al., 1992) combined with the new in situ submersible observations at station 6 allow us to interpret the curved western ridge (dive 85), which is located in the axial part of the N20°E trending area, as the active tectonic northern arm of a large overlapping system between the N20°E and N–S spreading axis. Several N5°E wide open faults occur in the central and eastern area, however, that could be interpreted as the initial stage of the northward propagation of the N–S spreading axis. The whole set of observations therefore indicates a very low volcanic accretion in this area.

South of latitude 18°10′S, the overlap with the N–N5°E southern pattern is very apparent (Figs. 3 and 4). The southern end of the N20°E spreading domain displays the characteristics of a typical

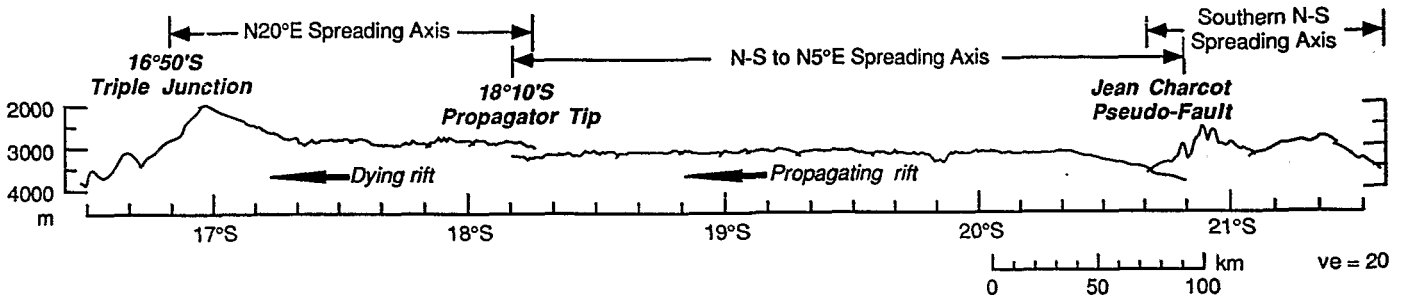

Fig. 8. Along-strike bathymetric profile from 21°30'S to 16°30'S.

large and evolutionary overlapping feature. West of the V-shape region, between 18°30'S and 18°00'S a 60 km long curved ridge rises about 300 m above the abyssal plain. Its concave eastward shape clearly resembles that of an Overlapping Spreading Center (OSC) volcanic tip (Fig. 5). Three other older OSC ridges, although less prominent, can be identified southwestward (Figs. 3 and 5); the westernmost (and oldest) OSC relict is partially incorporated in a large volcanic complex at 19°S.

The N to N5°E domain

The N–N5°E spreading axis extends for 280 km, from 18°10'S to 20°30'S. It is divided in two second order segments, defined by a slight change of the overall tectonic fabric of the area, including the present day axis trend, which changes from N–S in the southern part to N5°E in the northern part. This change takes place at 19°50'S.

North of 19°50'S, the tectonic fabric of the spreading axis parallels the N5°E structural trends, that consist of a succession of N5°E elongated horsts and grabens. The axial morphology is typical of an intermediate to fast spreading ridge system with a central dome, 5 to 8 km across, which is slightly elevated with respect to the NFB seafloor (200–300 m); locally an axial graben, a few tens to a few hundred meters wide, and a few tens of meters deep, can be observed. At its northern end, the axial N5°E domain bends progressively westward and deepens by about 300 m, near the intersection with the N20°E axis (Figs. 3 and 4). A small scale left lateral OSC occurs near 19°18'S, that is the single transform feature observed along this part of the axis. Along strike bathymetry (Fig. 8) shows a very smooth axial profile except for an axial rise of about 100–200 m, some 50 km long, and centered at 19°30'S approximately at the middle of the segment.

The most striking feature of the area is the presence of a broad inverse V-shaped region defined by the tectonic fabric at the northern end of the N–N5°E spreading ridge, which is characteritic a large northward propagating rift (Ruellan et al., 1992; De Alteriis et al., 1993). Moreover, the youngest structural trends, inside the N20°E axial domain, suggest a northward propagation of the N–N5°E axial trends beyond the northern tip of propagator. The northern tip of this zone separates two very different bathymetric, magnetic and tectonic patterns. A structural asymmetry can be observed inside the V-shaped region. The area west of the N5°E axis displays oblique and slightly curved morpho-tectonic lineations, whereas we can observe partially fitted in westward bending structures on the eastern side of the ridge.

Diving sites, located near 18°50'S (station 14) and at 19°S, in the middle of the wide flat dome that forms the spreading axial region, shows that the spreading axis is characterized by a narrow and V-shaped graben, 20 to 30 m deep and 40 to 50 m wide. It is bounded by two active normal fault scarps. Inside the graben are found drained lava lakes containing many remaining many pillars and large collapsed panels. Away from the axis we observe sheet flows and lobate lavas. Outside of the graben lies a succession of large areas covered with intact pillow lavas (without any fracturing), sheet flows and brecciated lavas. Hydrothermal biological communities are located primarily inside the axial graben, especially on the hollow lobate lava blisters, that are characterized by active vents inside fractures and spectacular dead chimneys (Auzende et al., 1992; Ondréas et al., 1993; Gràcia

et al., 1994-this issue). The hollow lobate lava blisters are unstable and collapse, inducing the dying of the biological communities.

Unlike the N20°E spreading domain, many large volcanic seamounts are associated with the N–N5°E spreading domain. They are mainly located off axis and tend to conceal the tectonic lineations. The sizes of the volcanoes are highly variable, ranging from a basal diameter of 4–5 km to more than 20 km and a height from 200 to even more than 1300 m (above the basin floor). Some of these volcanoes exhibit calderas (up to 1–2 km in diameter) indicating collapse of magmatic chambers (Batiza and Vanko, 1983). Most of these volcanoes, especially the larger ones, are built off-axis and distributed along eight alignments. No symmetry can be observed in the location of these seamounts or chains of seamounts with respect to the present day spreading axis. Four parallel and slightly curved chains, three very large and one small one, are located west of the ridge axis making an angle of 70° with the trend of the ridge. Four other chains, are located east of the axis, without any symmetry with the western ones and are aligned almost perpendicular to the ridge axis.

The older domains

The *N30°W domain* is located just east and northeast of the propagator V-shaped area, and east of the N 20°E domain. The topography is quite smooth compared with the axial domains previously described. This structural domain consists mainly of horsts and grabens trending N30°W, widely covered by sediments.

The *N30°E very complex domain* lies in the upper left corner of the structural map, west of N20°E axial domain. Two kinds of striking structural features coexist. The larger ones are N30°E lineaments defining two long horsts. The second one are complex curved structures located between the two N30°E trending horsts.

A small local *N–S domain* appears in the northeast corner of the structural map, east of the N 20°E domain and northeast of the propagating rift. The oceanic bottom is slightly elevated compared to the N20°E axial area. Both the oceanic structures and the magnetic anomalies are trending N–S.

Discussion

As previously described, the overall tectonic fabric of the axial domain strongly differs on both axis at the junction of the N–N5°E and N20°E segments, between 18° and 19° S (Figs. 3 and 5). Two main oceanic features are combined in this area: the large propagator at the northern end of the N–N5°E spreading ridge, and the large overlapping spreading center (OSC) at the southern end of the N20°E spreading domain.

The propagating rift of 18°10'S

The existence of propagating systems, occurring at divergent plate boundaries when the transform offset migrates has been widely demonstrated on the ocean floor (Shih and Molnar, 1975; Hey, 1977; Hey and Vogt, 1977; Hey et al., 1980; Gente, 1987). Nevertheless systematic observations are lacking. Only the 95.5°W Galapagos ridge area has been studied in detail, based on the analysis of Sea-Beam, GLORIA, Deep-Tow, seismology, magnetometry and gravity data (Hey and Vogt, 1977; Hey et al., 1980, 1986; Milholland and Duennebier, 1982; Searle and Hey, 1983; Phipps Morgan and Parmentier, 1985, 1987; Cooper et al., 1987; Kleinrock and Hey, 1989).

From the study of of the Galapagos propagator, Hey et al. (1980) first proposed a continuous propagation model with no overlap between the two axis, assuming that the spreading rate at the propagator tip is instantaneously at full speed, as the failing rift dies. On the basis of the observations of deformations of the lithosphere on Sea-Beam data and deep-tow survey also, Hey et al. (1986) later modified this model to incorporate a broad transform zone between overlapping propagating and failing rift axes. In that model, this broad shearing zone produces typically curved features at the tip of the propagator (Kleinrock and Hey, 1989).

In the North Fiji Basin, the observations of sea floor topography at the intersection between the N–N5°E and N20°E axes as described above, confirm the hypothesis of an active northward propagating system, between 18°S and 19°S (Ruellan et al., 1990, 1992; De Alteriis et al., 1993).

The propagation system produces a northward migration of the transform offset between the N–N5°E and N20°E axes. The active tip of the propagator is presently located at 18°10′S–173°33′E (Figs. 9 and 10).

Generally, most of the interpretations of oblique or bending lineations associated with propagating rift refer either to the pseudofaults (Hey and Vogt, 1977; Hey et al., 1980, 1986) which offset different magnetic patterns. or to the smaller scale pseudofaults inferred from detailed bathymetric, as in the case of the 95.5°W Galapagos propagator tip

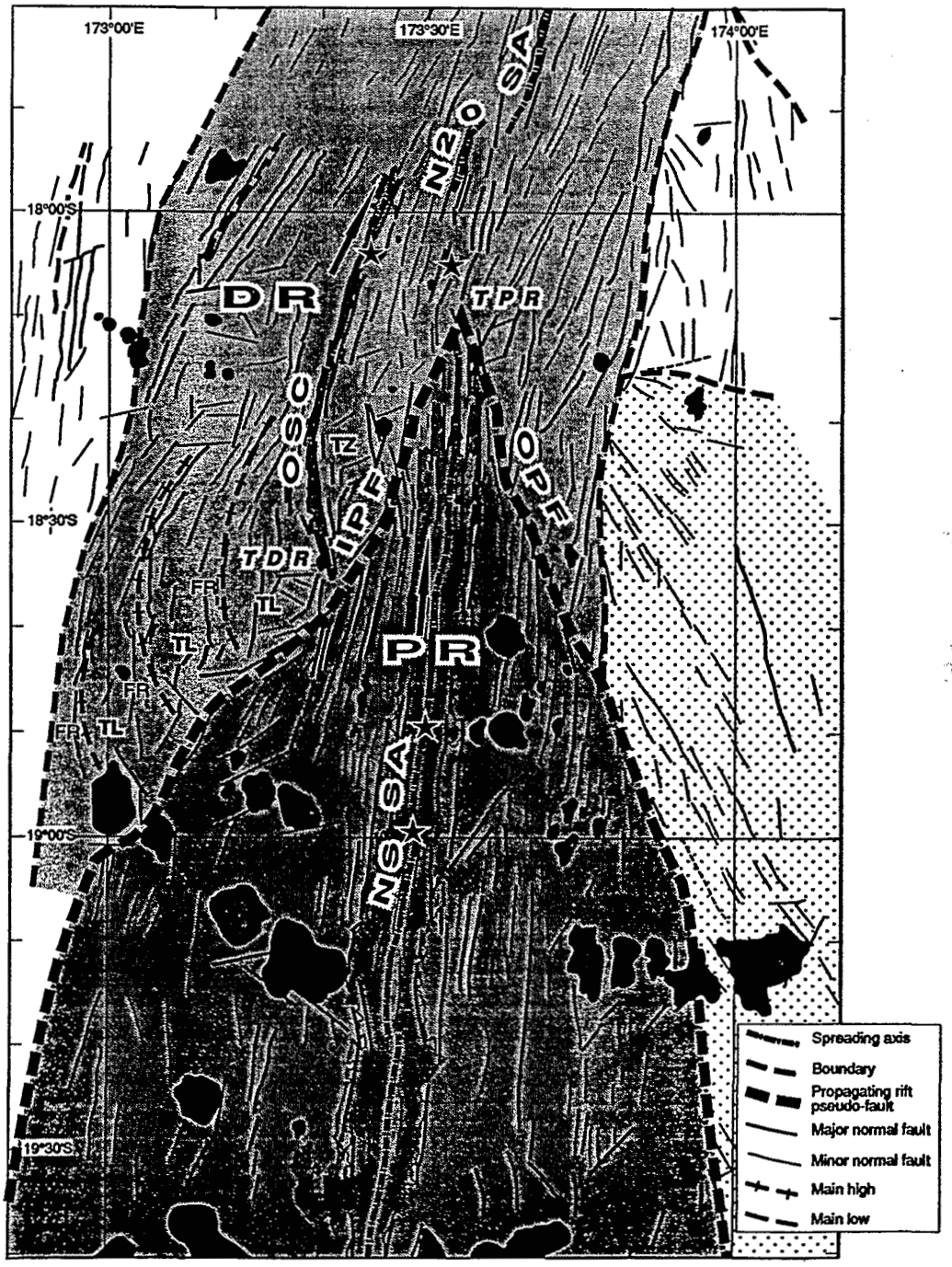

Fig. 9. The tectonic domains. *DR*=dying rift; *FR*=failed rift; *IPF*=inner pseudo-fault; *N20 SA*=N20°E spreading axis; *NS SA*=N–S spreading axis; *OPF*=outer pseudo-fault; *OSC*=overlapping spreading center; *PR*=propagating rift; *TDR*=active tip of the dying rift; *TL*=transferred lithosphere; *TPR*=tip of the propagating rift; *TZ*=transform zone. Stars indicate the diving sites and off-axis volcanoes appear in black.

Fig. 10. Tectonic pattern matched with the digital elevation model (DEM) of the propagating rift (Ifo–Khoros–Istar processing). *DR* = dying rift; *FR* = failed rift; *IPF* = inner pseudo-fault; *N20 SA* = N20°E spreading axis; *NS SA* = N–S spreading axis; *OPF* = outer pseudo-fault; *OSC* = overlapping spreading center; *PR* = propagating rift; *TDR* = active tip of the dying rift; *TL* = transferred lithosphere; *TPR* = tip of the propagating rift; *TZ* = transform zone.

(Kleinrock and Hey, 1989). It is important to note that the morphologic lineations are generally quite parallel inside the V-shaped domain bordered by the pseudofaults in the Galapagos propagator tip, whereas, in the case of NFB propagator, slightly oblique and curved patterns in the tectonic fabric appear in the western and eastern part of the V-shaped region respectively. Moreover, the gene-

ral shape of the whole propagator tip, inside of the V-shaped domain, is also slightly curved (Figs. 9 and 10).

This asymmetric tectonic fabric can be easily explained by a progressive migration in a constant N5°E direction of the curved overlapping segment of the N–N5°E ridge through time. The asymmetric oblique lineations are generated by tectonic deformation inside the broad shear zone lying between the N–N5°E axis and its counter part on the N20°E spreading ridge, i.e. inside the northward migrating overlapping area. This migration will leave behind oblique and curved structures as relict traces of older stages of the overlapping segment.

The propagating rift system is delimited by two external lines which represent respectively the inner and the outer pseudofaults of the propagation (Fig. 9). These lines are defined by the northern end of roughly N to N5°E parallel tectonic pattern in the abyssal hill fabric and by a succession of deep rhombic grabens. Subsequent changes in orientations of the pseudofaults lines, which are rather symmetric on each side of the axis, suggest that different phases either of propagation or/and spreading, characterized by different velocities has developed inside the V-shaped area. This analysis is also confirmed by the more or less elongated shape of the associated rhombic grabens.

The overlapping spreading center

The curved OSC ridge located at 18°30′S, in the N20°E domain, lies opposite the propagating rift segment (Fig. 9), that is also slightly curved and dip northward. The overlap with the N–N5°E spreading axis is 40 km long and the offset is 15 km. The offset is quite small and this tectonic pattern differs considerably from Galapagos ridge example. Moreover, from diving observations, the OSC ridge pertaining to the N20°E segment is clearly a magmatic rather than an amagmatic ridge, recording now a dominant tectonic activity. These evidences and the difference of trend of the two axis confer a quite original OSC configuration of the N–N5°E–N20°E spreading axes junction, and contrasts with the observation of Macdonald (1989) that propagating rifts are magmatically starved and severely tectonized, whereas the failing rifts are magmatically robust with little tectonic deformation. In the case of NFB central spreading ridge, the N–N5°E propagating rift is magmatically very active whereas the failing rift is strongly tectonized but magmatically starved.

In this configuration, the three southeastern curved highs of Fig. 9 may be interpreted as older abandoned Overlapping Spreading Centers tips belonging to the N20°E axis. Therefore, these relict tectonic features testify that the N20°E segment was longer in the past. It probably extended at least up to 19°S, to the southern end of the western most oldest ridge.

The transform zone and the transferred lithosphere

As defined by Hey et al. (1986), the transform zone consists of a broad area of active tectonic deformation located between the present day active arms of the overlapping spreading centers. In the case of the 18°10′S ridge junction (Figs. 9 and 10), almost all of the area between the inner pseudofault and the active N20°E curved arm displays positive reliefs with oblique N70°E to N85°E structural trends. Similar relief with oblique structural trends lies to the southeast, between the relict curved arms and the inner pseudofault, that could be interpreted as fossil transform zones which now pertain to the transferred lithosphere. These deformed zones were transferred from the East NFB plate to the West NFB as each spreading axis jump occurred. Thus, all the space between the older overlapping failed rifts and the present active one constitutes a domain of transferred lithosphere.

Tectonic model for the propagation of the N–S spreading axis since 1.8 Ma

The main questions arising from this kind of tectonic feature, that combines a prominent propagating rift with a wide overlapping spreading center concern its beginning and its stability through time and space.

A semi-quantitative model of the recent evolution (1.8 Ma to the present) of the N–N5°E and N20°E segments of the NFB ridge between 17°S

and 20°S is shown in Fig. 11. The N–N5°E axis, between 18°10′S and 20°30′S, represents the propagating segment of the ridge. It lengthens northward generating a V-shaped propagator and parallel lineations in the abyssal hills fabric. At stage 1, 1.8 Ma (anomaly 2), the opening of the NS segment at 19°30′S has just started whereas the N20°E one records only extensional tectonic features, such as open faults and fractures. At this stage, an offset seems to occur between the two segments but overlap probably does not occur. Note that at this time the N20°E segment was more N–S trending than now. At stage 2, spreading along the N20°E axis starts between magnetic anomalies 2 and J, while the N–N5°E axis continues or at least begins its northward propagation, penetrating the older N30°W trending tectonic domain. This propagation therefore induces the overlap of the two segments, and causes the first offset of the spreading axis to appear. At stage 3 (0.7 Ma), the offset between the two overlapping ridges becomes too large and unstable, and the western arm jumps backward to the northeast, from its initial position to a new position closer to the northern tip of the propagator. To the north, the second offset of the N20°E spreading axis occurs, and the N–S ridge now propagates into an area created by the N20°E spreading axis itself. From stage 3 to the present, the western arm jumps backward to the northeast twice again, following the continuous propagation of the N–S segment.

In view of the general V shape of the propagator and considering that the spreading rate of the N–S spreading axis is 6.9 cm/yr at 19°20′S and 6.6 cm/yr at 18°30′S (Huchon et al., 1994-this issue), we calculate the amount of lengthening and the velocity of propagation of the N–N5°E axis (Figs. 11 and 12). Since 1.8 Ma (magnetic anomaly 2), the N–N5°E axis has lengthened by about 103 km, from 19°04′S to its present day tip located at 18°09′S. From this lengthening, we deduce an average velocity of propagation of about 5.7 cm/yr, since 1.8 Ma. In this scenario, the local changes of the shape of the outer and inner-pseudofaults of the propagator, that are slightly asymmetric, must be considered as the result of variation of the propagation velocity, inside the V-shaped area. Assuming that the spreading rate remains rather homogeneous since 1.8 Ma, between 5.1 cm/yr (from anomaly 2 to anomaly J) and 7.6 cm/yr (from anomaly J to present) any widening of the V shape would indicate a slowing down while any narrowing of the V shape would underline an acceleration, in which case the calculated propagation velocity would have to range from 4.5 to 18 cm/yr. Looking at the propagator shape, we observe a recent pronounced acceleration of the propagation.

In contrast, the failing N20°E axis, between 18°10′S and the 16°50′S triple junction, shortens and probably reorients itself as occurs both the northward propagation of the N–N5°E arm and the evolution of the 16°50′S triple junction. Assuming that the original intersection of the two axes was close to the southern end of the oldest western OSC relict ridge (Fig. 11), a northeastward migration of the OSC must have occurred since about 1–1.8 Ma. Since anomaly J chron, the N20°E arm of the overlapping jumps northeastward three times, with an average velocity of 5.8 cm/yr, which is very close to the propagation velocity of the N–N5°E axis ridge.

A tentative model of kinematic evolution and predicted magnetic anomaly pattern is shown in Fig. 12. A constant spreading rate was used for each axis, as well as for the propagation rate. This model displays a theoretical ridge configuration that is compatible with the one observed (Fig. 11). The main difference lies in the fact that the theoretical magnetic anomaly model (Fig. 12) shows no overlap between the two spreading ridges. The explanation for this difference between the theoretical model and the observed magnetic and tectonic patterns is that the overlapping part of the N20°E arm is a transient feature which accommodates its original position for a period of time after the northward propagation of the N–N5°E segment occurs. From that model, we can define a particular trend which is the "failed rift line" (FRL) (Fig. 12), and which has been described previously by Hey et al. (1980, 1986) as the "failing rift" (FR). In the case of the NFB propagator, this line is not located at the tip of each identified overlapping arms (either the present one or the failed rift ones). It is located at the maximum curvature of each overlapping ridge. Thus, this failed rift line should be considered

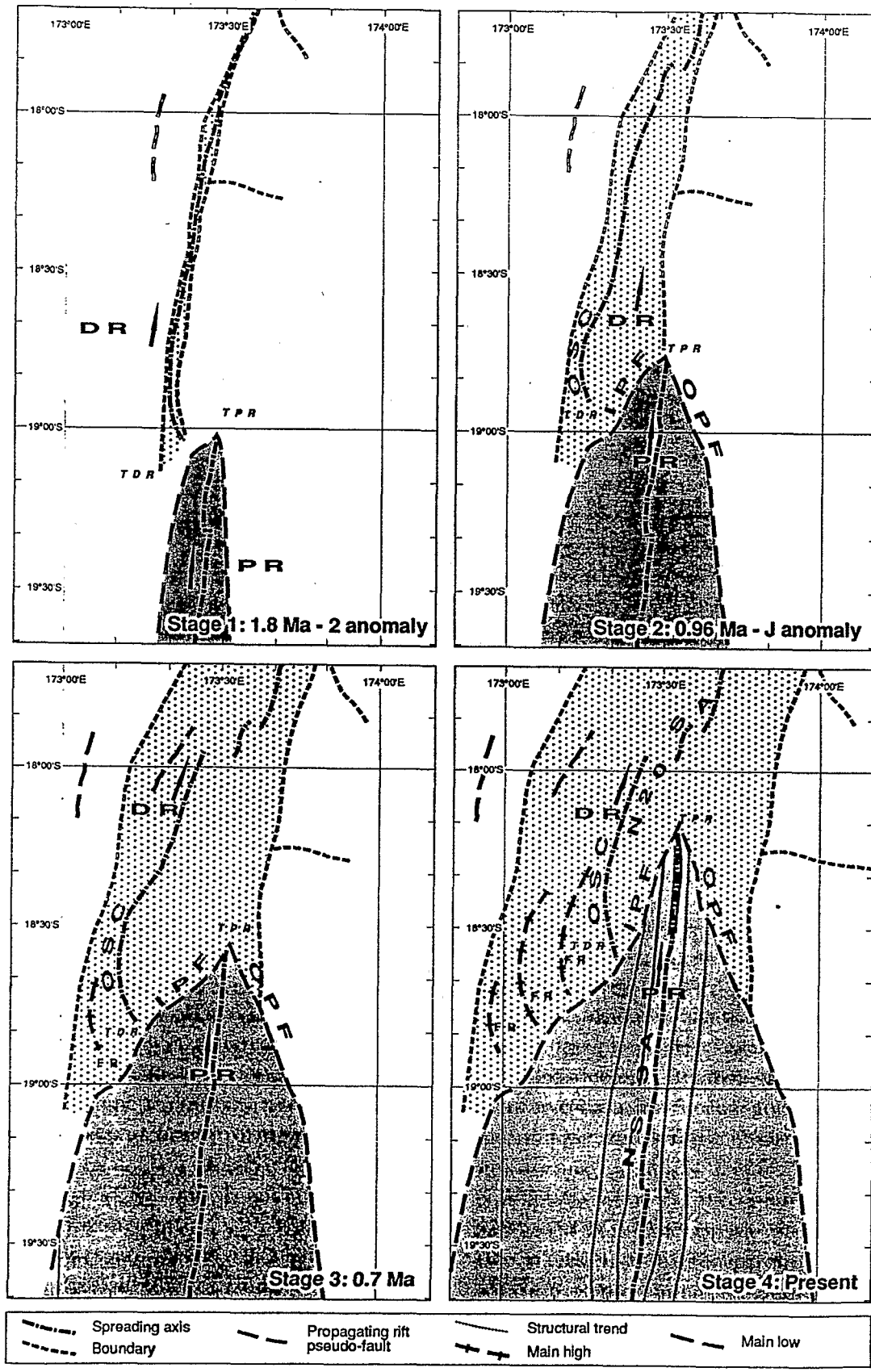

Fig. 11. Tentative evolution model of the propagating rift. While restoring the original segmentation of N–S and N20°E axes in the last 2 Ma, no changes in the orientation of N20°E axis have been considered, the offset and the overlap between axes have been kept rather constant through time. Abbreviations as in Figs. 10 and 11.

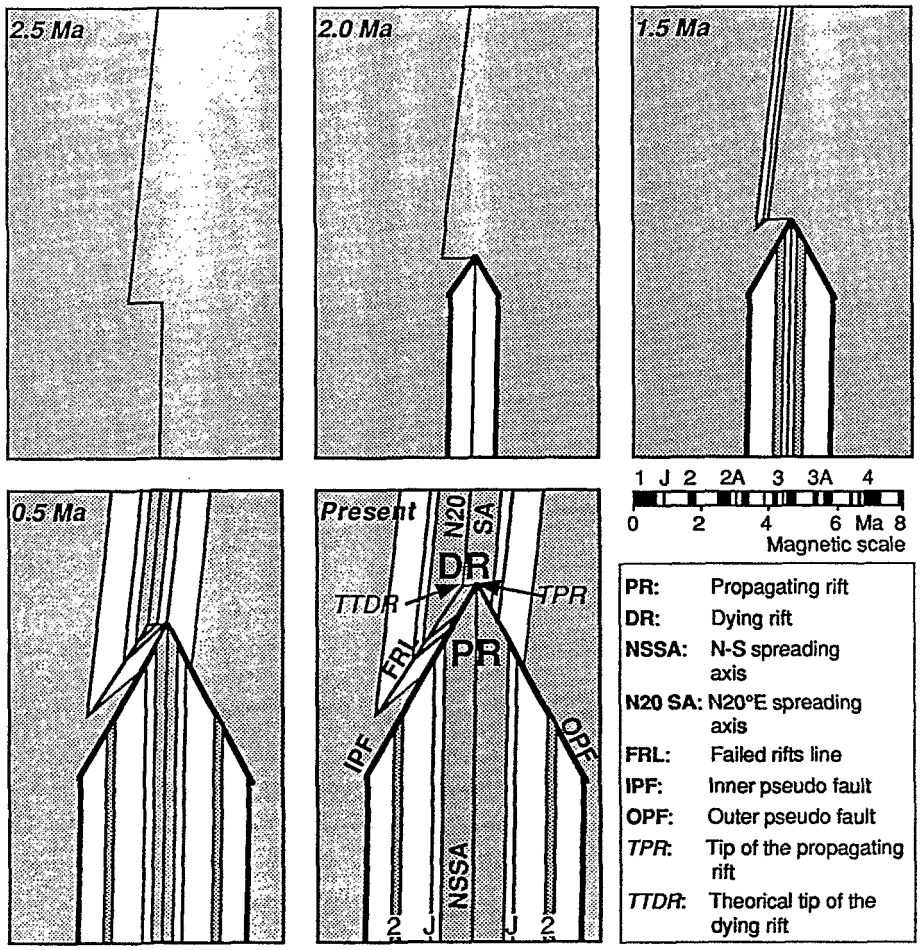

Fig. 12. Model of kinematic evolution and predicted magnetic anomaly pattern. A different orientation of the propagating and ailing axis has been introduced. An angle of 15° has been considered between the N–N5°E axis and the N20°E axis. Note that *FRL* and *IPF* are converging toward the propagator tip.

is the vector of the step by step northeast migration of successive overlapping arms pertaining to the N20°E ridge through time, responding each time by a jump of the axis to the increasing tectonic constrains produced by the northward propagation of the N–N5°E arm. Finally, noting that the 8°10′S NFB ridge junction is characterized by a difference of 15° between axial trends and by an outer overlap of the N20°E dooming rift, we can observe a slight convergence of the failed rift line FRL) with the inner pseudofault (IPF) and the northern propagator tip (TPR) in the model Fig. 12). This convergence could mean that the geodynamic evolution is progressively leading to a more simple spreading ridge configuration between the 16°50′S triple junction and the southern end of the N–N5°E axis, which might eventually result in single N5°E to N10°E ridge axis.

Conclusions

One of the most striking features of the North Fiji marginal basin is the propagating rift with overlapping spreading centers of 18°10′S. These kind of tectonic features were previously illustrated mainly on the Galapagos ridge and East Pacific Rise, respectively. The data presented above indicate that the spreading ridge system in the central part of the North Fiji Basin has evolved many times resulting in a complex ridge configuration composed of several segments that differ in length, orientation, segmentation, morphology, spreading rates, and magmatism and tectonic activity. The present intersection of the N20°E and N–N5°E axis is characterized by a transient feature related to the ongoing evolution of the ridge configuration. The NFB spreading system between 16°50′S and

21°S presently consists of two ridge segments with different lengths (280 km vs. 140 km) and orientations (N–N5°E vs. N20°E). The intersection of the two segments is characterized by a relatively large offset and overlap of the two axes. The present day magmatic and tectonicaly active N–N5°E spreading axis is located between 18°10'S and 20°30'S and is propagating northward to the detriment of the N20°E axis which is less active at its southern end. In the last 1.8 Ma, at least, the N–N5°E segment, slightly longer, has propagated northward with an average velocity of 5.7 cm/yr, whereas the N20°E one shortens itself at the same speed. The NFB propagator shows some similarities with the 95.5°W Galapagos propagator but also some major differences. The two NFB spreading axes have different orientations that may generate asymmetric structures near the transform zone. The sizes of overlap and offset between the two NFB axes, which are about 45 km and 20–25 km, respectively, differ considerably from those of 95.5°W Galapagos propagator (i.e. zero to a few kilometers for the overlap and 35–40 km for the offset respectively; Kleinrock and Hey, 1989). The NFB spreading system appears to be highly unstable, and rapidly evoluting resulting in considerable deformation of the ridge axis.

Acknowledgements

We are grateful to all the officers, crew, technical and scientific staffs who took part to the Japanese–French STARMER Project, as well as its funding agencies. We thank also Nathalie Pisot and Laurent Renouard from ISTAR Co., Georges Buffet and Laurent Nault from CNRS–URA *Géodynamique*, Jean-Patrick Giacometti and Patrick Cipière from INRIA–Sophia for their significant contribution on software development (IFO Project) and data processing. We thank Hélène Ondréas and Marc Sosson for their helpful comments and discussions. We thank the anonymous reviewers for their helpful detailed corrections on the manuscript. This work was supported with the founding of CNRS–INSU (France) and IFREMER (France). Contribution of *Institut de Géodynamique* (URA 1279 CNRS–UNSA).

References

Auzende, J.M., Eissen, J.P., Lafoy, Y., Gente, P. and Charlou, J.L., 1988a. Seafloor spreading in the North Fiji Basin (Southwest Pacific). Tectonophysics, 146: 317–351.

Auzende, J.M., Lafoy, Y. and Marsset, B., 1988b. Recent geodynamic evolution of the North Fiji Basin (SW Pacific). Geology, 16: 925–929.

Auzende, J.M., Honza, E., Boespflug, X., Deo, S., Eissen, J.P., Hashimoto, J., Huchon, P., Ishibashi, J., Iwabuchi, Y., Jarvis, P., Joshima, M., Kisimoto, K., Kiuwahara, Y., Lafoy, Y., Matsumoto, T., Maze, J.P., Mitsuzava, K., Momma, H., Naganuma, T., Nojiri, Y., Ohta, S., Otsuka, K., Okuda, Y., Ondreas, H., Otsuki, A., Ruellan, E., Sibuet, M., Tanahashi, M., Tanaka, T. and Urabe, T., 1990. Active spreading and hydrothermalism in North Fiji basin (SW Pacific). Results of Japanese–French cruise Kaiyo 87. Mar. Geophys. Res., 12: 269–283.

Auzende, J.M., Tanahashi, M., Bendel, V., Fujikura, K., Geistdoerfer, P., Gràcia-Mont, E., Joshima, M., Kisimoto, K., Mitsuzawa, K., Murai, M., Nojiri, Y., Ondreas, H., Pratt, C. and Ruellan, E., 1992. Résultats préliminaires des plongées du Shinkai 6500 sur la dorsale du Bassin Nord-Fidjien (SW Pacifique)—Programme STARMER. C. R. Acad. Sci. Paris, Sér. II, 314: 491–498.

Batiza, R. and Vanko, D., 1983. Volcanic development of small oceanic central volcanoes on the flanks of the East Pacific Rise inferred from narrow-beam echo-sounder surveys. Mar. Geol., 54: 53–90.

Chase, C.G., 1971. Tectonic history of the Fiji plateau. Geol. Soc. Am. Bull., 82: 3087–3110.

Cooper, P.A., Milholland, P.D. and Duennebier, F.K., 1987. Seismicity of the Galapagos 95.5°W propagating rift. J. Geophys. Res., 92: 14091–14112.

De Alteriis, G., Ruellan, E., Auzende, J.M., Ondréas, H., Bendel, V., Gràcia-Mont, E., Lagabrielle, Y., Huchon, P. and Tanahashi, M., 1993. Propagating rifts in the North Fiji basin (Southwest Pacific). Geology, 21: 583–586.

Gente, P., 1987. Etude morphostructurale comparative de dorsales océaniques à taux d'expansion variés. Schéma d'évolution morphologique de l'axe des dorsales; Liaison avec l'hydrothermalisme. Doct. Thesis Univ. Bretagne Occidentale, Brest, 373 pp.

Gill, J.B. and Gorton, M., 1973. A proposed geological and geochimical history of eastern Melanesia. In: P.J. Coleman (Editor), The Western Pacific: Islands Arcs, Marginal Seas, Geochemistry. Univ. Western Australia Press, pp. 543–566.

Gràcia, E., 1991. Etude morphostructurale du segment N160 de la dorsale du Basin Nord-Fidjien. Analyse des données de la campagne Yokosuka 90. Rapport de D.E.A., Univ. Bretagne Occidentale, Brest, 65 pp.

Gràcia, E., Ondréas, H., Bendel, V. and STARMER Group, 1994. Multi-scale morphologic variability of the North Fiji basin ridge. In: J.-M. Auzende and T. Urabe (Editors), North Fiji Basin: STARMER French–Japanese Program. Mar. Geol., 116: 133–151.

Harland, W.B., Armstrong, R.L., Cox, A.V., Craig, L.E., Smith, A.G. and Smith, D.G., 1990. A Geologic Time Scale 1989. Cambridge Univ. Press, 263 pp.

Hey, R., 1977. A new class of "pseudofaults" and their bearing on plate tectonics: a propagating rift model. Earth Planet. Sci. Lett., 37: 321–325.

Hey, R.N. and Vogt, P.R., 1977. Spreading center jumps and sub-axial astenosphere flow near the Galapagos hotspot. Tectonophysics, 47: 41–52.

Hey, R.N., Dunnebier, F.K. and Morgan, W.J., 1980. Propagating rifts on mid-ocean ridges. J. Geophys. Res., 85: 2647–2658.

Hey, R.N., Kleinrock, M.C., Miller, S.P., Atwater, T.M. and Searle, R.C., 1986. Sea-Beam/Deep-Tow investigation of an active oceanic propagting rift system, Galapagos 95.5°W. J. Geophys. Res., 91: 3369–3393.

Hey, R.N., Menard, H.W., Atwater, T.M. and Caress, D.W., 1988. Changes in direction of seafloor spreading revisited. J. Geophys. Res., 93: 2803–2811.

Huchon, P., Gràcia, E., Ruellan, E., Joshima, M. and Auzende, J.-M., 1994. Kinematics of active spreading in the central North Fiji basin (SW Pacific). In: J.-M. Auzende and T. Urabe (Editors), North Fiji Basin: STARMER French–Japanese Program. Mar. Geol., 116: 69–87.

Kleinrock, M.C. and Hey, R.N., 1989. Detailed tectonics near the tip of the Galapagos 95.5°W propagator: how the litosphere tears and a spreading axis develops. J. Geophys. Res., 94: 13801–13838.

Lafoy, Y., 1989. Evolution géodynamique des bassins marginaux Nord Fidjien et de Lau (Sud-Ouest Pacific). Doct. Thesis, Univ. Bretagne Occidentale, Brest, 260 pp.

Lafoy, Y., Auzende, J.M., Gente, P. and Eissen, J.P., 1987. L'extremité occidentale de la zone de fracture Fidjienne et le point triple de 16°40S. Résultats du Leg III de la campagne SEAPSO du N.O. Jean Charcot (Décembre 1985) dans le bassin Nord Fidjien, SW Pacifique. C. R. Acad. Sci. Paris, Sér. II, 304: 147–152.

Lafoy, Y., Auzende, J.M., Ruellan, E., Huchon, P. and Honza, E., 1990. The 16°40S Triple Junction in the North Fiji Basin (SW Pacific). Mar. Geophys. Res., 12: 285–296.

Maillet, P., Eissen, J.P., Lapouille, A., Monzier, M., Baleivuanala, V., Butscher, J., Gallois, F. and Lardy, M., 1986. La dorsale active du bassin Nord Fidjien entre 20°00S et 20°53S: signature magnétique et morphologique. C. R. Acad. Sci. Paris, Sér. II, 302: 135–140.

Mac Donald, K., 1989. Propagating rifts exposed. Nature, 342: 740–741.

Mac Donald, K. and Fox, P.J., 1983. Overlapping spreading centers: a new kind of accretion geometry on the East Pacific Rise. J. Geophys. Res., 88: 9393–9406.

Mac Donald, K., Scheirer, D.S. and Carbotte, S.M., 1991. Mid-ocean ridges: Discontinuities, segments and giant cracks. Science, 253: 986–994.

Menard, H.W. and Atwater, T., 1968. Changes in direction of Sea Floor Spreading. Nature, 219: 463–467.

Menard, H.W. and Atwater, T., 1969. Origin of Fracture Zone topography. Nature, 222: 1037–1040.

Milholland, P. and Duennebier, F.K., 1982. Seismicity at the 95.5°W Galapagos propagating rift. EOS Trans., Am. Geophys. Union, 63: 1025.

Miller, S.P. and Hey, R., 1986. Three-dimensional magnetic modelling of a propagating rift. Galapagos 95°30W. J. Geophys. Res., 91: 3395–3406.

Ondréas, H., Ruellan, E., Auzende, J.M., Bendel, V., De Alteriis, G., Gràcia-Mont, E., Lagabrielle, Y. and Tanahashi, M., 1993. Variabilité morphostructurale à l'échelle kilométrique de la dorsale du Bassin Nord Fidjien: Exploration in situ du segment compris entre 18°50S et 19°S. C. R. Acad. Sci. Paris, Sér. II, 316: 115–122.

Phipps Morgan, J. and Parmentier, E.M., 1985. Causes and rate limiting mechanisms of ridge propagation: a fracture mechanics model. J. Geophys. Res., 90: 8603–8612.

Phipps Morgan, J. and Parmentier, E.M., 1987. Three dimensional gravity modelling of the 95.5°W propagating rift in the Galapagos spreading center. Earth Planet. Sci. Lett., 81: 289–298.

Renard, V. and Allenou, J.P., 1979. Le Sea-Beam, sondeur multifaisceaux du N.O. "Jean Charcot". Description, évaluation et premiers résultats. Rev. Hydrogr. Int., Monaco, LVI(1): 35–71.

Ruellan, E., Auzende, J.M. and the STARMER group, 1989. L'accrétion dans le Bassin Nord-Fidjien méridional. Premiers résultats de la campagne franco-japonaise STARMER/KAIYO 88. C. R. Acad. Sci. Paris, Sér. II, 309: 1247–1254.

Ruellan, E., Auzende, J.M. and Maillet, P., 1990. L'axe d'accrétion actif Nord–Sud du Bassin Nord-Fidjien au sud de 18°30'S. Soc. Geol. Fr., Séance spécialisée "Oceans". (Sophia-Antipolis, 6–7 Décembre 1990.) 63.

Ruellan, E., Auzende, J.M., Lagabrielle, Y. and Tanahashi, M., 1992. Propagating rift combined with overlapping spreading center in the North Fiji Basin. IGC 1992, Kyoto, Japan.

Schilling, J.G., Meyer, P.S. and Kingsley, R.H., 1982. Evolution of the Iceland hot spot. Nature, 296: 313–320.

Searle, R.S. and Hey, R.N., 1983. Gloria observations of the propagating rift at 95.5°W on the Cocos–Nazca spreading center. J. Geophys. Res., 88: 6433–6447.

Shih, J. and Molnar, P., 1975. Analysis and implications of the sequence of the ridge jumps that eliminated the Surveyor transform fault. J. Geophys. Res., 88: 4815–4822.

Vine, F.J. and Matthews, D.H., 1963. Magnetic anomalies over oceanic ridges. Nature, 199: 947–949.

Reprinted from

MARINE GEOLOGY

INTERNATIONAL JOURNAL OF MARINE GEOLOGY, GEOCHEMISTRY AND GEOPHYSICS

Marine Geology, 116 (1994) 37–56
Elsevier Science B.V., Amsterdam

Propagating rift and overlapping spreading center in the North Fiji Basin

Etienne Ruellan[a], Philippe Huchon[b], Jean-Marie Auzende[c,1] and Eulàlia Gràcia[c]

[a]*CNRS, URA 1279 Géodynamique, rue A. Einstein, Sophia Antipolis, F-06560 Valbonne, France*
[b]*CNRS, URA 1316, Laboratoire de Géologie, ENS, 24 rue Lhomond, F-75231 Paris Cedex 05, France*
[c]*IFREMER, DRO-GM, B.P. 70, F-29280 Plouzané, France*

(Received May 6, 1993; revision accepted July 29, 1993)